

DFT Study of 7-R-3methylquinoxalin-2(1H)-ones (R=H; CH₃; Cl) as Corrosion Inhibitors in Hydrochloric Acid

Z. El Adnani^{1,2}, M. Mcharfi¹, M. Sfaira^{2,*}, M. Benzakour¹, A.T. Benjelloun¹, M. Ebn Touhami³, B. Hammouti⁴, M. Taleb²

¹ Equipe de Chimie Informatique et Modélisation, Laboratoire d'Ingénierie des Matériaux, Modélisation et Environnement, LIMME, Faculté des Sciences Dhar El Mahraz, Université Sidi Mohammed Ben Abdellah, BP 1796 – 30000, Atlas – Fès, Morocco.

² Equipe de Matériaux et Traitement de Surfaces, Laboratoire d'Ingénierie des Matériaux, Modélisation et Environnement, LIMME, Faculté des Sciences Dhar El Mahraz, Université Sidi Mohammed Ben Abdellah, BP 1796 – 30000, Atlas – Fès, Morocco.

³ Laboratoire des Matériaux, Electrochimie et Environnement, Faculté des Sciences, Université Ibn Tofaïl, BP. 133 – 14000, Kénitra, Morocco.

⁴ LCAE-URAC18, Faculté des Sciences, Université Mohammed Premier, BP 717 – 60000, Oujda, Morocco.

*E-mail: msfaira@yahoo.com

Received: 9 June 2012 / Accepted: 28 June 2012 / Published: 1 August 2012

A theoretical study based on DFT methods at B3LYP/6-31G** level of theory, was carried out, by means of the GAUSSIAN 03 set of programs, on three recently reported quinoxaline derivatives as corrosion inhibitors in acidic media. The computational calculations were undertaken to obtain information about the relationships between the molecular and electronic structures of the studied inhibitors and their experimental corrosion inhibition efficiencies. The structural parameters, such as the frontier molecular orbital energies (E_{HOMO} and E_{LUMO}), gap of energy ΔE , the charge distribution, the absolute hardness η and softness σ , the fraction of electrons ΔN transferred from the quinoxaline derivatives to the metallic surface, the total negative charge TNC as well as some electronic parameters such as the Natural Populations and the Fukui functions were calculated and discussed. The behaviour of these organic molecules in the presence of water has facilitated the understanding of the corrosion inhibition process.

Keywords: DFT calculations; Quinoxaline corrosion inhibitors; Descriptors; Fukui functions; PCM model

1. INTRODUCTION

Corrosion is the destructive attack on metals or alloys by chemical or electrochemical reaction with their environment, resulting in enormous economic losses. Acids are the most corrosive solvent; they are widely used in industries such as pickling, cleaning, descaling. In such aggressive medium, the use of organic corrosion inhibitors is one of the most common, effective and economic methods to protect metals [1,2].

The inhibitory effect of an organic inhibitor is reinforced by the presence of heteroatoms such as sulphur, nitrogen and oxygen in its molecule which facilitates its adsorption on the mild steel surface following the sequence $S > N > O$. Former studies concluded that the adsorption on the mild steel surface depends mainly on the physicochemical properties of the inhibitor group such as the planarity of the system, the presence of multiple adsorption active centers with lone pair and, or π orbitals, the electronic density at the donor atom and the molecular size [3,4]. Therefore, the choice of effective inhibitors is based on their structure, their mechanism of action and their electron donating ability.

Many N-polycyclic organic compounds have been reported as good inhibitors for mild steel in very corrosive media which grant this class of organic compounds an important position in the experimental studies of corrosion inhibitors [5-8]. The quinoxaline ring is one of the N-polycyclic aromatic compounds that have been proved to be excellent corrosion inhibitors for mild steel in acidic media [1,9,10]. In this work, we introduce three newly quinoxaline derivatives resulting of the substitution in C7 position of the quinoxaline ring (Figure 1) by H, CH_3 and Cl functions, namely 3,7-dimethylquinoxalin-2(1H)-one (Me-Q=O), 3-methylquinoxalin-2(1H)-one (Q=O) and 7-chloro-3-methylquinoxalin-2(1H)-one (Cl-Q=O). These inhibitors have been recently studied experimentally and present very distinguishable experimental corrosion inhibition efficiencies as reported in [11,12].

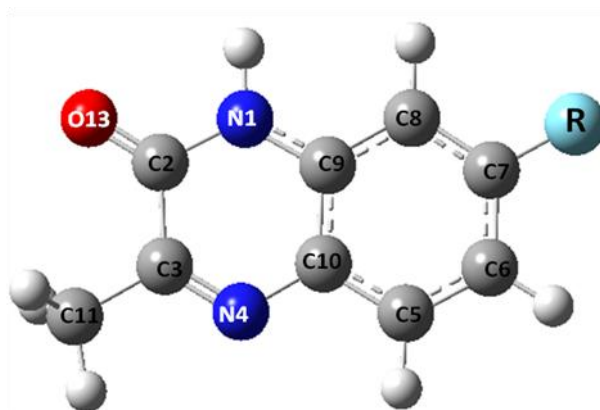


Figure 1. The 7-R-3-methylquinoxalin-2-one ring (R= CH_3 ; H; Cl)

Although experimental study of these molecules provide valuable information on their corrosion inhibition efficiency, a deep understanding of the inhibition property and mechanism remains crucial. Thus, theoretical methods have been introduced as novel, effective and inexpensive ways to evaluate the inhibition performance and/or to explain the inhibition mechanism. Among all

theoretical methods, quantum chemistry calculation has been widely used to study quantitatively the relationship between inhibition efficiency and molecular reactivity [13].

The main objective of this work is to investigate computationally, in gas and aqueous phases, using DFT at B3LYP/6-31G** level of theory, three recently synthesized quinoxaline derivatives Me-Q=O, Q=O and Cl-Q=O, in an attempt to find the most relevant theoretical parameters to characterize the inhibition properties of the inhibitors under study and to establish the correlation between their inhibition efficiency and their electronic as well as geometric properties.

2. CALCULATION METHODS

The quantum chemical calculations were performed on an Intel (R) core (TM)₂ Quad CPU (2.4 GHz and 8 GB RAM) workstation using standard Gaussian-03 software package [14] with complete geometry optimizations without constraints.

The geometry optimizations were carried out in gas phase at the Density Functional Theory (DFT) level using the hybrid functional B3LYP based on Becke's three-parameter functional including Hartree-Fock exchange contribution with a nonlocal correction for the exchange potential proposed by Becke [14,15] together with the nonlocal correction for the correlation energy provided by Lee et al. [16]. Indeed, DFT methods are often the methods of choice for similar calculations [15] because of their ability to overcome one of the main disadvantages of ab-initio methods; the complete neglect of electron correlation, by including some of it at greatly reduced computational cost [17]. Thus, all the parameters presented in this work were calculated at B3LYP with 6-31G** basis set for all atoms, frequently used for similar molecules [18-20].

Since the electrochemical corrosion takes place in the liquid phase; we found relevant to include the effect of solvent in the computations. Self-consistent reaction field (SCRF) theory [15], with Tomasi's polarized continuum model (PCM) [21], was used to perform the calculations in solution at B3LYP/6-31G** level, too. This method models the solvent as a continuum of uniform dielectric constant (ϵ) and defines the cavity where the solute is placed as a uniform series of interlocking atomic spheres. Since we cannot represent the implicit effect of hydrogen chloride solution, water is instead used to include the solvent effect [22].

The present study is undertaking the investigation of the existence of a clear relationship between the experimentally determined corrosion inhibition efficiencies of the studied inhibitors and a number of quantum-chemical parameters (descriptors) of the molecular reactivity. Therefore, some of the needed parameters are directly extracted from the output files of Gaussian [13] (E_{HOMO} , E_{LUMO} , μ) when other ones require to be computed separately (IP , EA , ΔE , χ , η , \square , ΔN and TNC).

According to the Koopmans' theorem [23] for closed-shell molecules, ionization potential IP and electron affinity EA can be expressed as follows in terms of E_{HOMO} , E_{LUMO} , the highest occupied molecular orbital energy, and the lowest unoccupied molecular orbital energy, respectively:

$$IP = -E_{HOMO} \quad (1)$$

$$EA = -E_{LUMO} \quad (2)$$

When the values of IP and EA are known, one can determine through the following expressions the values of the absolute electronegativity χ , the absolute hardness η and the softness σ (the inverse of the hardness):

$$\chi = \frac{IP + EA}{2} \quad (3)$$

$$\eta = \frac{IP - EA}{2} \quad (4)$$

$$\sigma = \frac{1}{\eta} \quad (5)$$

Moreover, for a reaction of two systems with different electronegativities, the electronic flow will occur from the molecule with the lower electronegativity (the organic inhibitor) towards that of higher value (metallic surface), till the chemical potentials are equal [22]. Therefore the fraction of electrons transferred (ΔN) from the inhibitor molecule to the metallic atom was calculated according to Pearson electronegativity scale [22]:

$$\Delta N = \frac{\chi_{Fe} - \chi_{inh}}{2(\eta_{Fe} + \eta_{inh})} \quad (6)$$

Where χ_{Fe} and χ_{inh} denote the absolute electronegativity of Fe and the inhibitor molecule, respectively; η_{Fe} and η_{inh} denote the absolute hardness of Fe and the inhibitor molecule, respectively. A theoretical value for the electronegativity of bulk iron was used $\chi_{Fe} = 7$ eV and a global hardness of $\eta_{Fe} = 0$, by assuming that for a metallic bulk $IP = EA$ because they are softer than the neutral metallic atoms [23]. Another parameter that was considered and that can give us valuable information about the reactive behavior of the studied inhibitors is the Total Negative Charge (TNC) obtained by summing up all the negative charges within a molecule [24,25].

Net atomic charges have been obtained using the Natural Population Analysis (NPA) of Weinhold [26]. The natural bond orbital analysis allowed us to describe the bonding in terms of the natural hybrids centered on each atom. The population analysis has been performed on the neutral, cationic and anionic species at the same obtained optimized geometry of each inhibitor in order to determine the corresponding Fukui functions.

3. RESULTS AND DISCUSSION

3.1. Molecular geometry

The geometries of all the molecules considered in this work were fully optimized at DFT level of theory using a B3LYP functional together with 6-31 G** basis set in gaseous

phase and the absence of imaginary frequencies in the vibrational spectrum proves that the equilibrium structures correspond to the minima energy for each quinoxaline derivative. Moreover, the geometries were re-optimized in aqueous phase at the same level of theory using PCM model for a better approach of the experimental parameters. The final geometries are given in Figure 2.

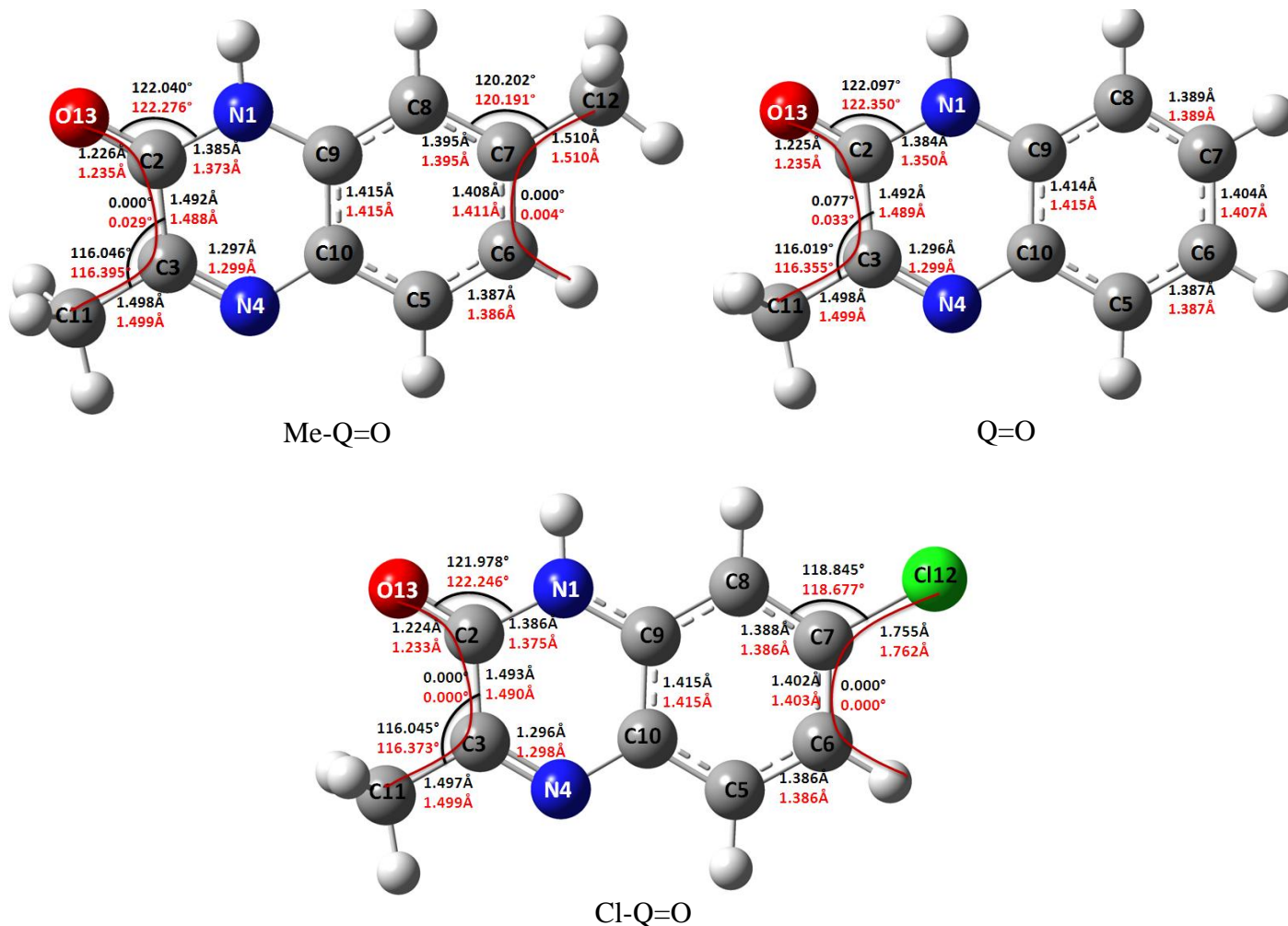


Figure 2. The selected geometrical parameters of the optimized studied quinoxaline derivatives calculated at B3LYP/6-31G** in gas (black) and aqueous phases (red)

It is observed from the computational results of the geometrical parameters that the nature of the substitution in C7 doesn't have appreciable effect on the structural parameters such as bond distances, bond angles and dihedral angles of the studied inhibitors.

Moreover, the bond lengths within the phenyl ring agree well with the expected values [27], except for the C9-C10 bonds (~ 1.415 Å) which are longer than the others probably because C9 and C10 are linked to N1 and N4 of the pyrazine ring respectively. The variations in the length of C2=O13 bonds were in agreement with the length of typical carbon oxygen double bond (~ 1.225 Å) [27] in gas phase. The C2-N1 single bond distances (~ 1.385 Å) were shorter than typical carbon nitrogen single bonds (1.42-1.47 Å) in gas phase [28] reflecting strong π electron delocalization in the quinoxaline

rings [29]. The average bond length of C3-N4 was (1.297 Å), indicating the existence of a double bond [30].

The solvent effect on the structural parameters is almost insignificant which is probably due to the planarity of the quinoxaline ring. However, a lengthened of C2=O13 (~1.235Å) and C7-Cl12 (~1.762Å) bond distances is noted in solution which is probably a result of the high polarity of these bonds [31]. Hence, the oxygen and the chlorine atoms will probably be more disposed to adsorb onto the mild steel surface.

3.2. Global molecular reactivity

The frontier orbitals (Highest Occupied Molecular Orbital, HOMO) and (Lowest Unoccupied Molecular Orbital, LUMO) of chemical species are very important in defining their reactivity. Fukui was the first to recognize this purpose [32]. The literature showed that the adsorption of the inhibitor onto the mild steel surface can occur on the basis of donor-acceptor interaction between the π electrons of the heterocyclic compounds and the vacant d orbitals of the mild steel surface atoms [3,4].

It is well recognized that the adsorption of the organic inhibitors can take place through the physical adsorption (physisorption) and/or the chemical adsorption (chemisorption) depending on the adsorption strength. When chemisorption takes place, the fact that one of the reacting species acts as an electron pair donor when the other reactant acts as an electron pair acceptor, gives the frontier molecular orbitals an important role in the understanding of the corrosion inhibition phenomena. E_{HOMO} is often associated with the electron donating ability of the molecules. Therefore, inhibitors with high values of E_{HOMO} have a tendency to donate electrons to appropriate acceptor with low empty molecular orbital energy. The obtained values of E_{HOMO} shown in Table 1 and represented in Figure 3(a), show that the substitution of the H atom in position C7 of Q=O by the methyl function in Me-Q=O (Figure 1) increases the value of the E_{HOMO} , on the other hand the substitution in position C7 by the chlorine group in Cl-Q=O decreases considerably the value of E_{HOMO} . These results can be explained by the electron releasing ability of the methyl group which may increase the electron donating ability of Me-Q=O and thereby its corrosion inhibition efficiency. Following the same logic the electron withdrawing effect of the chlorine group may be responsible for the decrease of the electron donating ability of Cl-Q=O and with it its corrosion inhibition efficiency. The E_{LUMO} describes the ability of the molecule to accept electrons, and the lowest its value the higher the capability of accepting electrons. Since good inhibitors are those who can accept as well as donate electrons to the metallic surface, we expected its values to decrease with the increase of inhibitive efficiencies of the studied inhibitors. However, the computed E_{LUMO} are in total disagreement with the experimental inhibition efficiencies as shown in Table 1 and represented in Figure 3(b). Thus, E_{LUMO} seems not to be a good descriptor to be taken into account to develop information about the corrosion inhibition phenomena within the studied molecular group.

The gap between the HOMO and LUMO energy levels of the molecules, $\Delta E = E_{LUMO} - E_{HOMO}$, is another important descriptor that should be considered [32]. Large values of the energy gap imply

high electronic stability resulting in low reactivity, when low values imply that it will be easier to remove an electron from the HOMO orbital to LUMO which can result in good inhibition efficiency.

Table 1. Quantum chemical descriptors of the studied inhibitors calculated at B3LYP/6-31 G** level of theory in gas (G) and in aqueous (A) phases and the experimental inhibition efficiencies

Inhibitor	Phase	E _{Total} a.u.	E _{HOMO} eV	E _{LUMO} eV	ΔE eV	\square D	IE% [11,12]
Me-Q=O	G	-571.863	-6.066	-1.659	4.407	3.626	81
	A	-571.881	-6.066	-1.686	4.380	5.318	
Q=O	G	-532.542	-6.174	-1.713	4.461	3.079	75.6
	A	-532.561	-6.120	-1.713	4.407	4.734	
Cl-Q=O	G	-992.135	-6.392	-1.958	4.434	1.212	56.5
	A	-992.154	-6.256	-1.850	4.406	2.039	

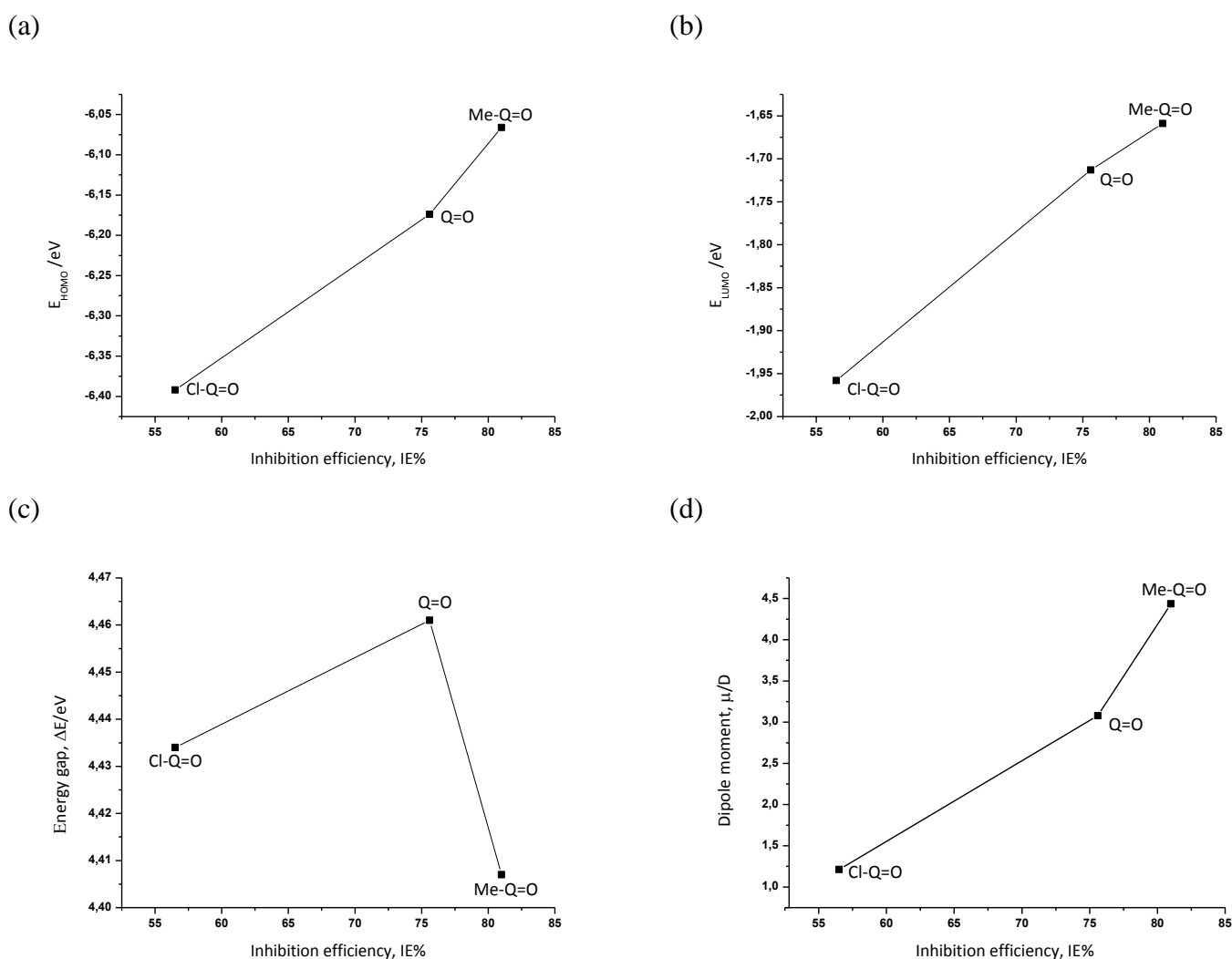


Figure 3. Correlation between the quantum chemical descriptors of the studied inhibitors calculated at B3LYP/6-31 G** level of theory in gas phase and the experimental inhibition efficiencies (a): E_{HOMO} , (b): E_{LUMO} (c): ΔE and (d):

The results presented in Table 1 and represented in Figure 3(c) show that Me-Q=O have the lowest energy gap 4.408 eV, therefore, its high reactivity can allow it to be easily adsorbed onto the mild steel surface leading to increase its inhibitive efficiency when compared to Cl-Q=O.

The values of the dipole moment displayed in Table 1 and represented in Figure 3(d), are the measurement of polarity within the entire molecules [33]. It is an index usually used for the prediction of the direction of a corrosion inhibition. Hence, it is generally agreed that the adsorption of polar compounds possessing high dipole moments on the mild steel surface should lead to better inhibition efficiency [34]. The results show that Me-Q=O have the highest value of dipole moment 3.626D with respect to Q=O and Cl-Q=O with values of 3.079 D and 1.212 D, respectively. Consequently, we can assume that the adsorption of Me-Q=O onto the metallic surface will be stronger than those of Q=O and Cl-Q=O, and thus the corresponding inhibition efficiency will follow the order Me-Q=O > Q=O > Cl-Q=O. These results are in good agreement with the experimental outcomes.

The electronegativity and the global hardness indicate the molecular capability of accepting electrons then the smaller their values, the higher their ability of donating electrons. It could be seen from their calculated values shown in Table 2 and represented in Figure 4(a,b), that Me-Q=O have the lowest electronegativity and the lowest hardness values indicating the high reactivity of Me-Q=O compared to Cl-Q=O which can explain its high corrosion inhibition efficiency.

The fraction of electrons transferred ΔN describes the trend of electrons donation within a set of inhibitors. According to Lukovits study [35], if $\Delta N < 3.6$ then the inhibition efficiency increased with increasing electron-donating ability at the mild steel/electrolyte interface. The obtained values of ΔN reported in Table 2 are all below 3.6 and the results show that the substitution of the methyl function by the chlorine function in C7 lead to a notable decrease in ΔN values. Agreeing with these results, the calculations show that the value of the Total Negative Charge (*TNC*) of Me-Q=O is higher than these of Q=O and Cl-Q=O respectively, thus, Me-Q=O will exhibit better adsorption onto the mild steel surface increasing its inhibition efficiency.

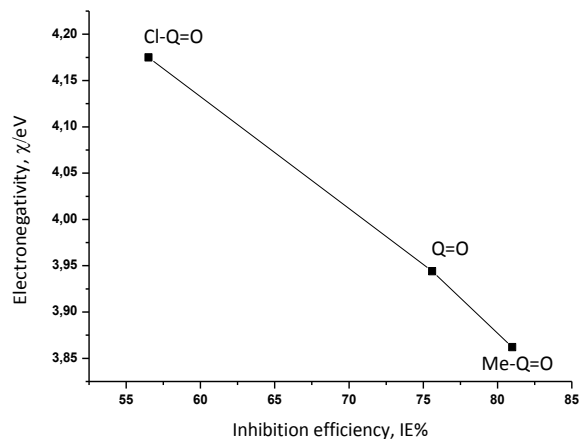
The evolution of most of the global investigated descriptors may be explained by the electronic effect of the substituent in the C7 position; i.e., the fact that the substituent is directly linked to the benzene ring is probably responsible for the adsorption strength on the metallic surface. Indeed, the electron releasing effect (+I) of the methyl into the benzene ring is probably improving its ability to donate electrons resulting in better reactivity as corrosion inhibitor; when the electron withdrawing inductive effect (-I) of the chlorine is reducing its reactivity [36-37]. Hence Me-Q=O would have better disposition to donate its electrons resulting with stronger adsorption onto the mild steel surface, and, in turn is Q=O and Cl-Q=O.

From the computed results in gas and aqueous phases (Tables 1 and 2), we can easily notice the stabilization effect of solvent in the significant decrease of the Total Energy (E_T), values of all three inhibitors. Also, we can detect the enhancement of their reactivity in aqueous phase given that the values of ΔE and η decrease considerably in aqueous phase. We can also observe the increase in the values of μ , ΔN as well as *TNC* which indicate a higher disposition of the inhibitors to donate their electron; hence a better adsorption onto the mild steel surface [38].

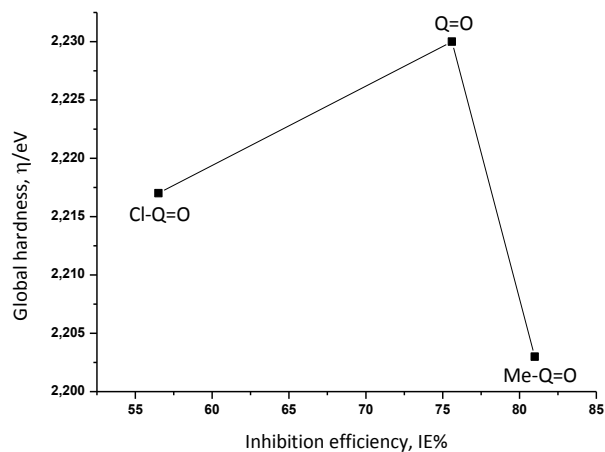
Table 2. Quantum chemical descriptors of the studied inhibitors calculated at B3LYP/6-31G** level of theory in gas (G) and in aqueous (A) phases and the experimental inhibition efficiencies

Inhibitor	Phase	IP eV	EA eV	χ eV	η eV	σ eV	ΔN eV	TNC	IE% [11,12]
Me-Q=O	G	6.066	1.659	3.862	2.203	0.454	0.712	2.800	81
	A	6.066	1.686	3.876	2.190	0.457	0.713	2.985	
Q=O	G	6.174	1.713	3.944	2.230	0.448	0.685	2.635	75.6
	A	6.120	1.713	3.917	2.203	0.454	0.699	2.635	
Cl-Q=O	G	6.392	1.958	4.175	2.217	0.451	0.637	2.414	56.5
	A	6.256	1.850	4.053	2.203	0.453	0.668	2.715	

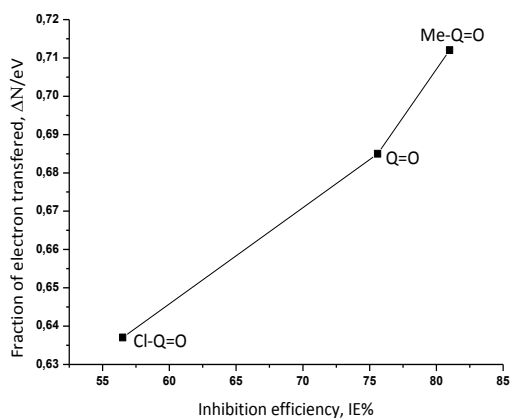
(a)



(b)



(c)



(d)

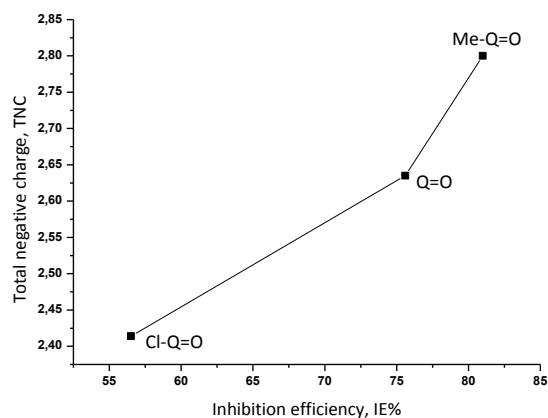


Figure 4. Correlation between the quantum chemical descriptors of the studied inhibitors calculated at B3LYP/6-31 G** level of theory in gas phase and the experimental inhibition efficiencies (a): χ , (b): σ , (c): ΔN and (d): TNC

The almost uniform electron density distribution of the frontier orbitals shown in Figure 5 implies that the absorption will probably occur on multiple reactive sites distributed along the molecular structure, which may increase the adsorption stability and led to the improvement of inhibition efficiency of the studied inhibitors.

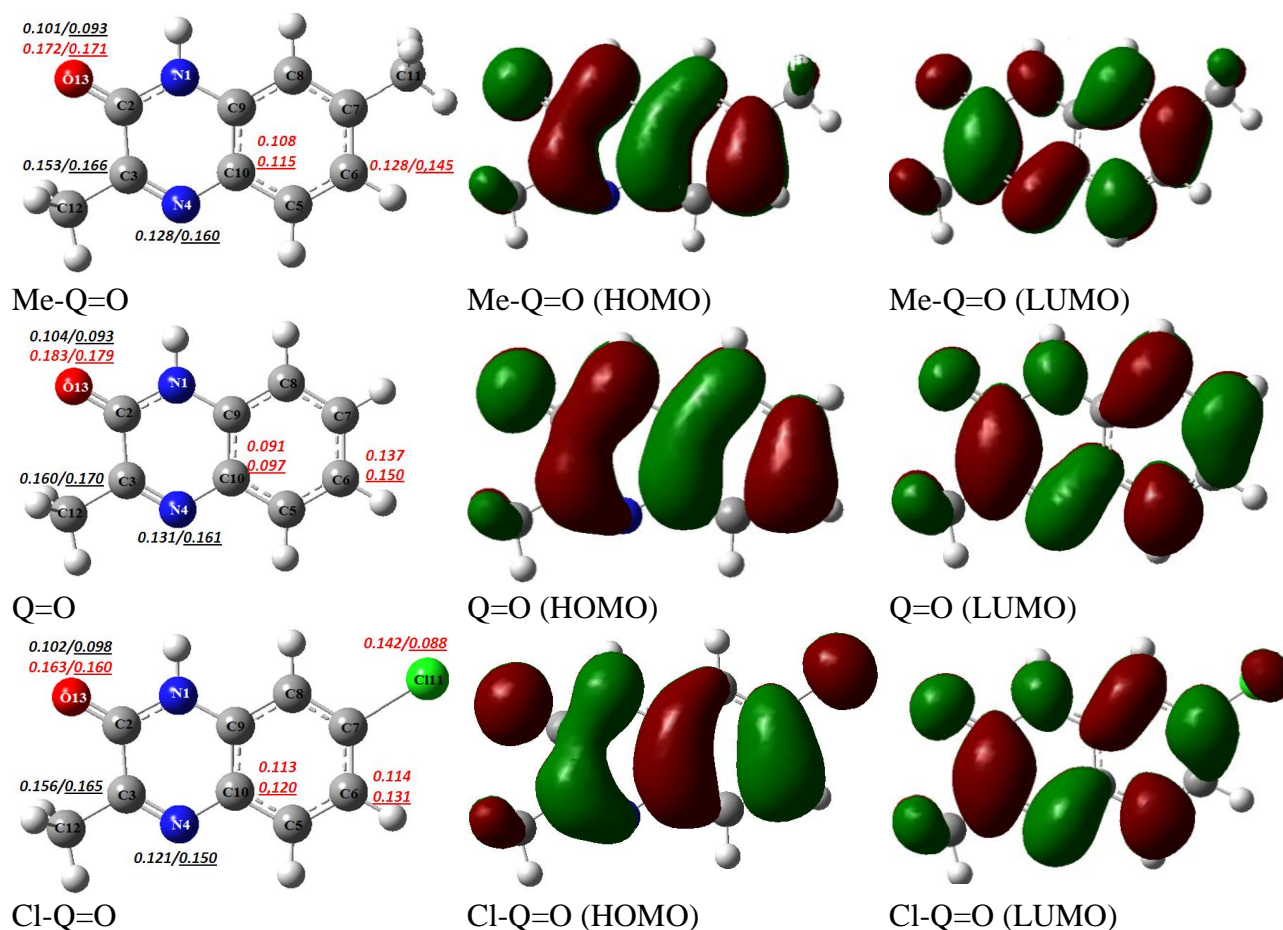


Figure 5. Fukui functions (f_k^+ : black, f_k^- : red, *italic*: gas phase, underline: aqueous phase), the HOMO and the LUMO of Me-Q=O, Q=O and Cl-Q=O computed at B3LYP/6-31G** level in gas phase

3.3. Local molecular reactivity

To get some insight into the local reactivity of the studied inhibitors, the Fukui functions were computed since they are the relevant reactivity indicators in the electron-transfer controlled reactions such as corrosion inhibition process [37,39]. Their values are used to identify which atoms in the inhibitors are more prone to undergo an electrophilic or a nucleophilic attack.

For a system of N electrons, independent single-point calculations were made for corresponding $N+1$ and $N-1$ electron systems.

Table 4. Pertinent natural populations and Fukui functions of the studied inhibitors calculated at B3LYP/6-31G** in gas (G) and aqueous (A) phases

Inhibitor	Atom	Phase	PN	PN+1	PN-1	fk+	fk-	fk0
Me-Q=O	N1	G	7.593	7.630	7.527	0.037	0.066	0.051
		A	7.587	7.641	7.417	0.054	0.170	0.112
	C3	G	5.800	5.953	5.716	0.153	0.084	0.118
		A	5.800	5.966	5.720	0.166	0.08	0.123
	N4	G	7.417	7.545	7.366	0.128	0.051	0.089
		A	7.439	7.599	7.511	0.160	0.072	0.044
	C6	G	6.255	6.266	6.127	0.011	0.128	0.069
		A	6.261	6.274	6.116	0.013	0.145	0.079
	C7	G	6.004	6.099	5.925	0.095	0.079	0.087
		A	6.005	6.080	5.980	0.075	0.025	0.050
	C10	G	5.902	5.887	5.794	-0.015	0.100	0.046
		A	5.907	5.898	5.792	-0.009	0.115	0.053
	O13	G	8.609	8.710	8.437	0.101	0.172	0.136
		A	8.673	8.766	8.502	0.093	0.171	0.132
Q=O	N1	G	7.592	7.632	7.510	0.040	0.082	0.061
		A	7.586	7.642	7.496	0.056	0.090	0.073
	C3	G	5.796	5.956	5.721	0.160	0.075	0.117
		A	5.796	5.966	5.727	0.170	0.069	0.119
	N4	G	7.418	7.549	7.393	0.131	0.025	0.078
		A	7.439	7.600	7.415	0.161	0.024	0.092
	C6	G	6.259	6.272	6.122	0.013	0.137	0.075
		A	6.265	6.278	6.115	0.013	0.150	0.081
	C7	G	6.213	6.311	6.154	0.098	0.059	0.078
		A	6.221	6.305	6.179	0.084	0.042	0.063
	C10	G	5.897	5.884	5.806	-0.013	0.091	0.039
		A	5.902	5.894	5.805	-0.008	0.097	0.044
	O13	G	8.607	8.711	8.424	0.104	0.183	0.143
		A	8.672	8.765	8.493	0.093	0.179	0.136
Cl-Q=O	N1	G	7.593	7.629	7.533	0.036	0.060	0.048
		A	7.586	7.638	7.509	0.052	0.077	0.064
	C3	G	5.794	5.950	5.706	0.156	0.088	0.122
		A	5.792	5.957	5.709	0.165	0.083	0.124
	N4	G	7.417	7.538	7.397	0.121	0.020	0.070
		A	7.437	7.587	7.415	0.150	0.022	0.086
	C6	G	6.272	6.284	6.158	0.011	0.114	0.069
		A	6.277	6.290	6.146	0.013	0.131	0.079
	C7	G	6.024	6.097	5.979	0.073	0.045	0.059
		A	6.030	6.096	5.984	0.066	0.046	0.056
	C10	G	5.900	5.888	5.787	-0.012	0.113	0.050
		A	5.900	5.895	5.780	-0.005	0.120	0.057
	Cl12	G	16.991	17.081	16.849	0.090	0.142	0.116
		A	17.006	17.070	16.918	0.064	0.088	0.076
O13	G	8.600	8.702	8.437	0.102	0.163	0.132	
	A	8.655	8.753	8.495	0.098	0.160	0.129	

The resulting natural population analysis yields to $P_k(N-1)$, $P_k(N)$, and $P_k(N+1)$, the population for all atoms k . In a finite-difference approximation the population analysis of atoms in molecules, depending on the direction of the electron transfer, then the condensed Fukui functions were computed using the following equations from the Exact Theory [40]:

$$f_k^+ = P_k(N+1) - P_k(N) \quad (\text{For nucleophilic attack}) \quad (7)$$

$$f_k^- = P_k(N) - P_k(N-1) \quad (\text{For electrophilic attack}) \quad (8)$$

$$f_k^0 = \frac{P_k(N+1) - P_k(N-1)}{2} \quad (\text{For radical attack}) \quad (9)$$

The calculated Fukui's functions for all the inhibitors are presented in Table 4 as well as the corresponding population for the neutral and ionic species. For simplicity, only the more significant values of the Fukui functions are presented. It can be noticed that the f_k^- values at O13, C6, and C10 atoms were the largest for all the three molecules (Table 4), which implied that these atoms are disposed to provide electrons to form coordinate bonds with the metal atoms. Hence these atoms will probably be the electrophilic reactive sites during the absorption. In addition to these three atoms, C112 in Cl-Q=O displays high value of f_k^- . As for f_k^+ , we found the largest values at C3, N4 and O13, which implied that these atoms will be the nucleophilic reactive sites probably able to accept electrons from metal atoms and, or to form back-donating bonds with the metal atoms. It is worth noting that from the Fukui functions results of C7 displays clearly the formerly discussed electronic effect of the substituent at this position. Hence, when we compare the C7 values of f_k^- we found that it respects the following order Me-Q=O > Q=O > Cl-Q=O indicating that the electron releasing effect of the methyl function enhance the nucleophilic character of Me-Q=O.

4. CONCLUSION

Using the DFT/B3LYP method with the 6-31G**, the molecular geometries and molecular relativities of three quinoxaline derivatives were investigated leading to the following conclusions:

1. Most of the studied quantum chemical descriptors are in excellent agreement with the experimental observations.
2. The substitution of the methyl function by the chlorine function in C7 leads to a notable decrease in the adsorption capacity of the inhibitors which is the result of the electronic effect of the substituent directly attached to the phenyl ring.
3. The solvent effect was clearly detected in the stabilization of the inhibitors, and also in the enhancement of their reactivity illustrate by the increase of μ , ΔN and TNC values and also by the decrease of ΔE , η values.

4. The Fukui functions and the electron density distribution show the existence of multiple reactive sites spread along the molecular structures probably leading to a strong adsorption on the metallic surface.

ACKNOWLEDGEMENTS

We are grateful to the “Association Marocaine des Chimistes Théoriciens” (AMCT) for its help concerning the Gaussian 03 program.

References

1. B. Zerga, R. Saddik, B. Hammouti, M. Taleb, M. Sfaira, M. Ebn Touhami, S.S. Al-Deyab, N. Benchat, *Int. J. Electrochem. Sci.* 7 (2012) 631.
2. M. Elayyachy, B. Hammouti, A. El Idrissi, A. Aouniti, *Portug. Electrochim. Acta*, 29 (2011) 57.
3. A.O. Yuce, G. Kardas, *Corros. Sci.*, 58 (2012) 86.
4. S. John, A. Joseph, *Mater. Chem. Phys.*, 133 (2012) 1083.
5. B. Zerga, A. Attayibat, M. Sfaira, M. Taleb, B. Hammouti, M. Ebn Touhami, S. Radi, Z. Rais, *J. Appl. Electrochem.*, 40 (2010) 1575.
6. M.B. Cisse, B. Zerga, F. El Kalai, M. Ebn Touhami, M. Sfaira, M. Taleb, B. Hammouti, N. Benchat, S. El kadiri, A.T. Benjelloun, *Surf. Rev. Lett.*, 18 (2011) 303.
7. S. Aloui, I. Forsal, M. Sfaira, M. Ebn Touhami, M. Taleb, M.F. Baba, M. Daoudi, *Portug. Electrochim. Acta*, 27 (2009) 599.
8. Z. El Adnani, M. Mcharfi, M. Sfaira, A.T. Benjelloun, M. Benzakour, M. Ebn Touhami, B. Hammouti, M. Taleb, *Int. J. Electrochem. Sci.*, 7 (2012) 3982.
9. N. Saoudi, A. Bellaouchou, A. Guenbour, A. Ben Bachir, E. M. Essassi, M. El Achouri, *Bull. Mater. Sci.*, 33 (2010) 313.
10. A. Zarrouk, B. Hammouti, R. Touzani, S.S. Al-Deyab, M. Zertoubi, A. Dafali, S. Elkadiri, *Int. J. Electrochem. Sci.*, 6 (2011) 4939
11. K. Adardour, O. Kassou, R. Tourir, M. Ebn Touhami, H. ElKafsaoui, H. Benzeid, El M. Essassi, M. Sfaira, *Mater. Environ. Sci.*, 1 (2010) 129.
12. K. Benbouya, B. Zerga, M. Sfaira, M. Taleb, M. Ebn Touhami, B. Hammouti, H. Benzeid, El M. Essassi, *Int. J. Electrochem. Sci.*, 7 (2012) submitted.
13. Gaussian 03, Revision B.01, M.J. Frisch, G.W. Trucks, H.B. Schlegel, G.E. Scuseria, M.A. Robb, J.R. Cheeseman, J.A. Montgomery Jr., T. Vreven, K.N. Kudin, J.C. Burant, J.M. Millam, S.S. Iyengar, J. Tomasi, V. Barone, B. Mennucci, M. Cossi, G. Scalmani, N. Rega, G.A. Petersson, H. Nakatsuji, M. Hada, M. Ehara, K. Toyota, R. Fukuda, J. Hasegawa, M. Ishida, T. Nakajima, Y. Honda, O. Kitao, H. Nakai, M. Klene, X. Li, J.E. Knox, H.P. Hratchian, J.B. Cross, C. Adamo, J. Jaramillo, R. Gomperts, R.E. Stratmann, O. Yazyev, A.J. Austin, R. Cammi, C. Pomelli, J.W. Ochterski, P.Y. Ayala, K. Morokuma, G.A. Voth, P. Salvador, J.J. Dannenberg, V.G. Zakrzewski, S. Dapprich, A.D. Daniels, M.C. Strain, O. Farkas, D.K. Malick, A.D. Rabuck, K. Raghavachari, J.B. Foresman, J.V. Ortiz, Q. Cui, A.G. Baboul, S. Clifford, J. Cioslowski, B.B. Stefanov, G. Liu, A. Liashenko, P. Piskorz, I. Komaromi, R.L. Martin, D.J. Fox, T. Keith, M.A. Al-Laham, C.Y. Peng, A. Nanayakkara, M. Challacombe, P.M.W. Gill, B. Johnson, W. Chen, M.W. Wong, C. Gonzalez, and J.A. Pople, *Gaussian, Inc., Pittsburgh PA*, 2003.
14. A.D. Becke, *Chem. Phys.*, 98 (1993) 5648.
15. A.D. Becke, *Phys. Rev. A.*, 38 (1988) 3098.
16. C. Lee, W. Yang, R.G. Parr, *Phys. Rev. B.*, 37 (1988) 785.
17. C.C. Zhan, J. A. Nichols, D.A. Dixon, *J. Phys. Chem. A*, 107 (2003) 4184.
18. N.O. Obi-Egbedi, I.B. Obot, *Corros. Sci.*, 53 (2011) 263.

19. P. Udhayakala , T.V. Rajendiran, *JCBPSC*, 2 (2012) 172.
20. P. Udhayakala, A. Jayanthi, T.V. Rajendiran, *Der Pharma Chemica*, 3 (2011) 528.
21. W. Wang, W.J. Mortier, *J. Am. Chem. Soc.*, 108 (1986) 5708.
22. K.F. Khaled, *Electrochim. Acta*, 22 (2010) 6523.
23. V.S. Sastri, J.R. Perumareddi, *Corrosion*, 53 (1997) 617.
24. S.E.Nataraja, T.V. Venkatesha, H.C. Tandon, B.S. Shylesha, *Corros. Sci.*, 53 (2011) 4109.
25. S.E.Nataraja, T.V. Venkatesha, H.C. Tandon, *Corros. Sci.* (2012),
<http://dx.doi.org/10.1016/j.corsci.2012.03.034>
26. (a) A.E. Reed, L.A. Curtiss, F. Weinhold, *Chem. Rev*, 88 (1988) 899. (b) P. Udhayakala, A. Jayanthi, T.V. Rajendiran, *Der Pharma Chemica*, 3 (2011) 528.
27. W.B. Schweizer, J.D. Dunitz, *Helv. Chem. Soc*, 65 (1982) 1547.
28. F.H. Allen, O. Kennard, D.G. Watson, L. Brammer, A.G. Orpen, R.J. Taylor, *Chem. Soc. Perkin Trans. 2*, (1987) S1.
29. G. Gece, S. Bilgiç, *Corros. Sci.*, 52 (2010) 3304.
30. J. Zhang, G. Qiao, S. Hu, Y. Yan, Z. Ren, L. Yu, Z. Ren, L. Yu, *Corros. Sci.*, 53 (2011) 147.
31. M. Mcharfi, *Thesis « Contribution à l'étude théorique et expérimentale des protéines : Cas des dipeptides Pro-Asx et Asx-Pro »*, Sidi Mohammed ben Abdellah University (2002).
32. K. Fukui, T. Yonezawa, H. Shingu, *J. Chem. Phys.*, 20 (1952) 722.
33. N.O. Eddy, S.R. Stoyanov, E.E. Ebenso, *Int. J. Electrochem. Sci.*, 5 (2010) 1127.
34. E.E. Ebenso, D.A. Isabiry, *Int. J. Mol. Sci.*, 11 (2010) 2473.
35. I. Lukovits, E. Kalman, F. Zucchi, *Corrosion*, 57 (2001) 3.
36. A. Yurt, G.B. Duran, H. Dal, *Arab. J. Chem.*, (2010), Doi:10.1016/j.arabjc.2010.12.010.
37. L. M. Rodriguez-Valdez, A. Martinez-Villafane, D. Glossman-Mitnik, *J. Mol. Struct.*, 48 (2006) 4053.
38. S. Safak, B. Duran, A. Yurt, G. Turkoglu, *Corros. Sci.*, 54 (2012) 251.
39. P.W. Ayers, R.G. Parr, *J. Am. Chem. Soc.* 122 (2000) 2010.
40. M.A. Quijano, M.P. Pardav, A. Cuán, M.R. Romo, G.N. Silva, R.Á. Bustamante, A.R. López, H.H. Hernández, *Int. J. Electrochem. Sci.*, 6 (2011) 3729.